

# Numerical and analytical methods for asymptotically flat spacetimes

**Oliver Rinne**

Max Planck Institute for Gravitational Physics (Albert Einstein Institute),  
Am Mühlenberg 1, 14476 Potsdam, Germany  
Department of Mathematics and Computer Science, Freie Universität Berlin,  
Arnimallee 2-6, 14195 Berlin, Germany  
E-mail: [oliver.rinne@aei.mpg.de](mailto:oliver.rinne@aei.mpg.de)

**Abstract.** This article begins with a brief introduction to numerical relativity aimed at readers who have a background in applied mathematics but not necessarily in general relativity. I then introduce and summarise my work on the problem of treating asymptotically flat spacetimes of infinite extent with finite computational resources. Two different approaches are considered. The first approach is the standard one and is based on evolution on Cauchy hypersurfaces with artificial timelike boundary. The well posedness of a set of constraint-preserving boundary conditions for the Einstein equations in generalised harmonic gauge is analysed, their numerical performance is compared with various alternate methods, and improved absorbing boundary conditions are constructed and implemented. In the second approach, one solves the Einstein equations on hyperboloidal (asymptotically characteristic) hypersurfaces. These are conformally compactified towards future null infinity, where gravitational radiation is defined in an unambiguous way. We show how the formally singular terms arising in a  $3 + 1$  reduction of the equations can be evaluated at future null infinity, present stable numerical evolutions of vacuum axisymmetric black hole spacetimes and study late-time power-law tails of matter fields in spherical symmetry.

*Submitted as the introductory chapter of a Habilitation thesis consisting of the published papers [1]–[6] to the Department of Mathematics and Computer Science at Freie Universität Berlin in November 2013*

This article is organised as follows. In section 1 we give an introduction to the basics of numerical relativity, with a focus on the Cauchy problem, formulations of Einstein’s equations and numerical methods. In section 2 we introduce the main subject of this thesis, the treatment of asymptotically flat spacetimes and the “outer boundary problem” in numerical relativity. Section 3 summarises my work on the first approach to this problem, namely Cauchy evolution with artificial timelike boundary. Section 4 is devoted to a different approach based on hyperboloidal evolution to future null infinity. Finally in section 5 we conclude and give a brief outlook on future research directions.

## 1. Numerical relativity

### 1.1. A brief history

Einstein's 1915 theory of general relativity has revolutionised the way we think about gravitation. Its radical difference from other field theories lies in the fact that its equations govern the geometry of spacetime itself, as opposed to most other theories where fields evolve on an unchanging background geometry. The geometry of spacetime is determined by its matter content through Einstein's field equations. In turn, matter moves along geodesics of this spacetime manifold. To put it simply, *gravitation is geometry*.

Through observations such as the perihelion shift of Mercury, the bending of light in the gravitational field of the sun, the gravitational redshift, and the decrease of the orbital period of binary pulsars consistent with the loss of energy due to emission of gravitational radiation (Hulse & Taylor, Nobel prize 1993), general relativity is by now one of the most accurately verified physical theories. Nevertheless, most of these observations only test the validity of the theory in the weak-field limit. Almost a century after Einstein's discovery, still relatively little is known about the full implications of the theory in the nonlinear regime.

Aside from these astrophysical questions, there are several problems in mathematical relativity that remain unanswered. Two of the most important ones are the question of black hole stability and the cosmic censorship conjecture. Even though widely expected to be true, it was only in 1993 that Christodoulou and Klainerman were able to prove in a voluminous work [7] that flat (Minkowski) spacetime is nonlinearly stable. Despite some recent progress, a similar theorem for the general stationary vacuum black hole, the Kerr solution, is still lacking. This is of central importance as black holes are believed to be ubiquitous in the universe.

A different conjecture, first put forward by Penrose in 1969 [8] and termed *cosmic censorship*, concerns the global behaviour of solutions. The Einstein equations are known to form singularities from quite general initial data [9]. The (weak) cosmic censorship conjecture states that (very roughly) any singularities formed from generic initial data lie inside an event horizon, i.e. they are causally disconnected from (invisible to) far-away observers. So far there is no general proof of this conjecture, which has important consequences on the determinism of the theory.

Why then do Einstein's equations pose such tremendous difficulties to the mathematician? Despite their elegant geometric origin, they turn out to be a complicated system of coupled nonlinear second-order partial differential equations (PDEs). Exact solutions are generally only known under strong simplifying assumptions such as the existence of spacetime symmetries. Small perturbations of known solutions can be studied by linearising the field equations.

One approach to studying the behaviour of more general solutions is the use of numerical approximations. Due to the complexity of the equations involved, this requires powerful computers, and as a result *numerical relativity* is a relatively young field of

research: it started around 1964 with pioneering work by Hahn & Lindquist [10], who studied the head-on collision of two black holes. Since then the field has had a history of several breakthroughs as well as long periods of struggle. (Excellent recent textbooks on the subject are for example [11, 12].)

Arguably one of the most important achievements made through numerical simulations is the discovery of critical phenomena in gravitational collapse by Choptuik in 1993 [13]. This was triggered by a question posed by a mathematical relativist (Christodoulou): consider a family of initial data corresponding to compact matter configurations with one parameter, such that for small values of the parameter the configuration will disperse to leave flat spacetime behind, whereas for large values it will collapse to form a black hole. What happens at the threshold between the two outcomes? Choptuik investigated this using sophisticated numerical methods (most importantly, adaptive mesh refinement) and observed phenomena similar to thermodynamic phase transitions, including power-law scaling of the black hole mass in supercritical evolutions and a universal, self-similar critical solution.

The majority of researchers in numerical relativity focused on what was regarded as the most important outstanding problem in numerical relativity, the collision of two orbiting black holes. Black holes being the simplest objects in general relativity, this is the obvious analogue of the two-body problem in Newtonian gravity. The problem received so much attention because binary black hole collisions are widely considered to be the strongest sources of gravitational waves, which are hoped to be detected directly in the near future by several earth-based detectors already in operation, a planned space-based detector (eLISA) that has just been approved by the European Space Agency to be launched in 2034, and alternative observational methods such as pulsar timing arrays. There is thus a strong need for models of gravitational waveforms from astrophysical events to be used for matched filtering in gravitational wave data analysis. Despite much effort spent on the binary black hole problem, it was not until 2005 that the final breakthrough was made and the first complete simulations of the inspiral, merger and ringdown of a black hole binary were presented almost simultaneously by three different groups [14, 15, 16]. By now such simulations have almost become routine. Wider regions of the parameter space have been explored, matter has been included (binary neutron stars or neutron star/black hole binaries) and more complicated physics is being added. These “numerical laboratories” serve as substitutes for experiments on astronomical scales—an interesting philosophical shift of paradigm.

### *1.2. The Cauchy problem for the Einstein equations*

In order to understand why the numerical solution of Einstein’s equations poses such difficulties, let us consider the general structure of these equations. Spacetime is described by a smooth four-dimensional manifold  $M$  with a smooth Lorentzian metric

$g_{ab}$ .<sup>‡</sup> The Einstein equations are

$$G_{ab} = \kappa T_{ab}. \quad (1)$$

Here  $G_{ab} = R_{ab} - \frac{1}{2}Rg_{ab}$  is the Einstein tensor,  $R_{ab}$  is the Ricci tensor and  $R$  the scalar curvature. These are evaluated with respect to the Levi-Civita connection compatible with  $g_{ab}$ . On the right-hand side,  $T_{ab}$  is the energy-momentum tensor describing the matter content of spacetime, and  $\kappa$  is a constant. For the time being we may assume vacuum,  $T_{ab} = 0$ . Equation (1) is to be solved for the metric  $g_{ab}$ ; it thus forms a system of second-order, quasi-linear PDEs. A key property of (1) is its invariance under arbitrary smooth transformations of the spacetime coordinates  $x^a$ , a principle often referred to as general covariance.

However, in order to solve the equations numerically, one needs to pick a particular coordinate chart in order to obtain a definite set of PDEs. This is most often done using the Cauchy or initial-value formulation of general relativity.<sup>§</sup> For this one picks a time coordinate  $t := x^0$  and considers a foliation of spacetime into the slices  $\Sigma(t)$  of constant time  $t$ . Indices  $i, j, \dots$  from the middle of the alphabet will be used to denote the spatial coordinates  $x^i$ ,  $i = 1, 2, 3$ . The Einstein equations (1) split into two different classes. The equations for which both indices are spatial ( $ab = ij$ ) are found to contain second time derivatives of the metric; these six equations are called *evolution equations*. The equations for which one index is temporal (say  $a = 0$ ) are found to contain no second time derivatives of the metric; these four equations are therefore called *constraint equations*. The constraint equations are preserved under the time evolution in the sense that if the constraints vanish at one instant of time then the evolution equations imply that their time derivatives vanish as well. This is a consequence of the contracted Bianchi identities

$$\nabla^b G_{ab} = 0, \quad (2)$$

where  $\nabla$  denotes the covariant derivative compatible with  $g_{ab}$ . While this is true on the analytical level, numerical simulations have long been plagued by exponentially growing constraint violations. Only relatively recently has this problem been cured (see below in section 1.3.1).

On an initial spacelike hypersurface  $\Sigma_0$  corresponding to  $t = 0$ , we specify initial data for  $g_{ab}$  and  $\partial_t g_{ab}$  satisfying the constraint equations. (Constructing such data is itself a highly nontrivial problem, see [18] for a review.) The evolution equations are then integrated forward in time in order to obtain  $g_{ab}$  for  $t > 0$ . There is a slight problem though: we have ten unknowns  $g_{ab}$  but only six evolution equations. At this point general covariance comes into play: fixing the coordinates allows us to impose four conditions on the components of  $g_{ab}$ , the so-called coordinate or *gauge* conditions.

<sup>‡</sup> Throughout we use abstract index notation, whereby  $g_{ab}$  represents the  $\binom{0}{2}$  tensor field  $g$  on  $M$ . Indices  $a, b, \dots$  range over  $0, 1, 2, 3$ . The notation in this chapter has been streamlined to be self-consistent; it differs from the notation used in some of the following chapters.

<sup>§</sup> A different approach is the characteristic formulation; see [17] for a review and also section 2.3 in this chapter.

Thus we really only have six free components of the metric that are evolved by the six evolution equations.

In a numerical simulation it is difficult if not impossible to fix the spacetime coordinates *a priori* as one does not usually know what spacetime a given set of initial data will evolve to. Instead one ties the coordinates to the dynamical fields, hoping that the coordinates that are thus being constructed “on the fly” will have desirable properties (e.g., avoidance of singularities). Depending on how this is done, the final set of PDEs one obtains may take on very different forms. In fact, the Cauchy problem may be well posed or ill posed! In the following subsection we briefly review the two formulations of the Einstein equations that are most often used in numerical relativity and, in fact, in the present thesis.

### 1.3. Formulations of the Einstein equations

*1.3.1. Generalised harmonic coordinates* One way to fix the spacetime coordinates is to impose a wave equation on each of the coordinates  $x^a$ :

$$\square x^a \equiv g^{bc} \nabla_b \nabla_c (x^a) = -g^{bc} \Gamma^a_{bc} = H^a, \quad (3)$$

where  $\Gamma^a_{bc}$  denotes the Christoffel symbols of the Levi-Civita connection. Such coordinates are called (*generalised*) *harmonic*. The source functions  $H^a$  on the right-hand side may depend on the coordinates  $x^a$  and on the metric  $g_{ab}$  but not on derivatives of the metric.

With this gauge condition the vacuum Einstein equations can be written as

$$g^{cd} \partial_c \partial_d g_{ab} = -\nabla_a H_b - \nabla_b H_a + 2g^{cd} g^{ef} (\partial_e g_{ca} \partial_f g_{db} - \Gamma_{ace} \Gamma_{bdf}), \quad (4)$$

i.e. the principal part of the equation becomes the d’Alembert operator associated with the metric. Hence the system of PDEs is symmetric hyperbolic, a fact that was used by Fourès-Bruhat in her celebrated proof of the well-posedness of the Cauchy problem for the Einstein equations [19].

Yet it was only much later that harmonic coordinates made their way into numerical relativity. Pretorius’ 2005 breakthrough binary black hole simulations [14] were based on this system.

A crucial ingredient was a new method to control the growth of constraint violations. In the generalised harmonic formulation, the role of the constraints is taken on by the quantities

$$\mathcal{C}^a := g^{bc} \Gamma^a_{bc} + H^a, \quad (5)$$

which must vanish for a solution to the Einstein equations because of the gauge condition (3). The evolution equation (4) implies the following evolution equation for the constraints:

$$\nabla^b \nabla_b \mathcal{C}_a + \mathcal{C}^b \nabla_{(a} \mathcal{C}_{b)} = 0. \quad (6)$$

|| Note the d’Alembert operator is meant to act on each of the coordinates as scalar functions here.

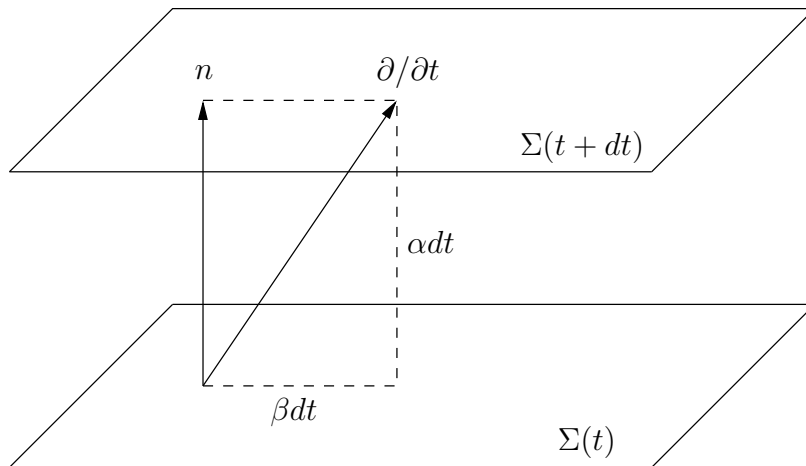


**Figure 1.** 3 + 1 decomposition with unit timelike normal  $n^a$ , lapse function  $\alpha$  and shift vector  $\beta^i$ .

A linear stability analysis of this equation shows that not all modes decay, and they may be amplified due to the nonlinearity of the equation. The key idea now is that we are still free to add multiples of the constraints  $\mathcal{C}_a$  to (4) because these vanish for a solution to Einstein's equations. Such terms will not affect the principal part of (4) because the constraints contain only first derivatives of the metric. Adding constraints to (4) will modify the constraint evolution equation (6). In [20] a particular combination of such *constraint damping terms* was devised such that on the linear level all non-constant modes of the modified constraint evolution equation decay.

The generalised harmonic formulation of the Einstein equations forms the basis of the first part of this thesis (chapters II–IV). More precisely, we use a first-order reduction (with respect to time and spatial derivatives) of (4) developed by the Caltech-Cornell numerical relativity collaboration. Details of this reduction can be found in [21] and in [1].

*1.3.2. ADM formulation* Before the introduction of generalised harmonic coordinates in numerical relativity, most numerical work was based on the 3+1 or *ADM formulation* of the Einstein equations originally developed by Arnowitt, Deser and Misner in 1962 with a view towards quantising gravity ([22]; see also [23]). In this framework one decomposes the vector field  $\partial/\partial t$  associated with the time coordinate  $t$  into a part normal to the hypersurface  $\Sigma(t)$  of constant  $t$  and a part tangential to it:

$$\left(\frac{\partial}{\partial t}\right)^a = \beta^a + \alpha n^a, \quad (7)$$

where  $n^a$  denotes the unit timelike normal to  $\Sigma(t)$ ,  $\alpha$  is the lapse function and  $\beta^i$  the shift vector¶(figure 1).

¶ Since  $\beta^a$  is tangential to  $\Sigma(t)$ , it has only three nonvanishing components, hence we write it as  $\beta^i$ .

The spacetime metric takes the form

$$g = -\alpha^2 dt^2 + \gamma_{ij}(dx^i + \beta^i dt)(dx^j + \beta^j dt), \quad (8)$$

where  $\gamma_{ij}$  is the spatial metric (first fundamental form) induced on  $\Sigma(t)$ . We also need to introduce the extrinsic curvature (second fundamental form)

$$K_{ij} = -\frac{1}{2}\mathcal{L}_n\gamma_{ij}, \quad (9)$$

where  $\mathcal{L}$  denotes the Lie derivative,  $\mathcal{L}_n = \alpha^{-1}(\partial_t - \mathcal{L}_\beta)$ . Equation (9) can be regarded as an evolution equation for  $\gamma_{ij}$ . The vacuum Einstein equations imply an evolution equation for  $K_{ij}$ ,

$$\mathcal{L}_n K_{ij} = -\alpha^{-1}D_i D_j \alpha + \mathcal{R}_{ij} - 2K_{ik}K^k_j + K_{ij}K, \quad (10)$$

where  $D$  denotes the covariant derivative compatible with  $\gamma_{ij}$ ,  $\mathcal{R}_{ij}$  is the Ricci tensor of  $\gamma_{ij}$ , and  $K = \gamma^{ij}K_{ij}$ . The constraint equations take the form

$$\mathcal{H} := \mathcal{R} + K^2 - K_{ij}K^{ij} = 0, \quad (11)$$

$$\mathcal{M}^j := D_i(K^{ij} - \gamma^{ij}K) = 0, \quad (12)$$

where  $\mathcal{R}$  is the scalar curvature of  $\gamma_{ij}$ .

It was only realised in the numerical relativity community in the 1990s that for fixed lapse and shift, the ADM evolution equations (9) and (10) are only weakly hyperbolic and hence the initial value problem is ill posed (see [24] for a review of hyperbolicity for the Einstein equations).

One way to cure this is to add multiples of the constraints, especially the momentum constraint (12), to (10). This was the essential trick that led to the formulation of Baumgarte, Shapiro, Shibata and Nakamura (*BSSN*) [25, 26], which in addition to the generalised harmonic formulation has become one of the two standard formulations used in binary black hole simulations.

A different approach, taken in the second part of this thesis, is the use of elliptic gauge conditions. As a condition on the spacetime slicing we shall require the mean curvature  $K$  of the slices to be a spacetime constant. Apart from its geometric appeal, this will furnish the desired asymptotic behaviour of the slices (see section 2.4). Such slices also have good singularity avoidance properties as the mean curvature controls the time evolution of the spatial volume element  $\sqrt{\det \gamma_{ij}}$ . Preservation of the constant mean curvature (CMC) condition under the time evolution leads to an elliptic equation for the lapse function  $\alpha$ . The spatial coordinates will be required to be *spatially harmonic*, i.e.,

$$\Delta x^i \equiv \gamma^{jk}D_j D_k(x^i) = -\gamma^{jk}{}^{(3)}\Gamma^i_{jk} = H^i, \quad (13)$$

where the  $H^i$  are fixed functions of the spatial coordinates (cf. (3)); now  ${}^{(3)}\Gamma^i_{jk}$  refers to the Christoffel symbols of  $\gamma_{ij}$ . Taking a time derivative of (13) results in an elliptic equation for the shift vector  $\beta^i$ . It has been shown at least in the spatially compact case that the ADM system with these elliptic gauge conditions (CMC slicing and spatially harmonic gauge) has a well-posed initial value problem [27]. The price to pay is that

we need to solve elliptic equations at each time step of the numerical evolution, which is generally more computationally expensive than solving hyperbolic equations.

As mentioned earlier, due to general covariance, there is a redundancy in Einstein's equations that allows one to solve only the evolution equations<sup>+</sup>; the constraints will be preserved under the time evolution. (Of course one still needs to check that violations of the constraints remain small during a numerical evolution.) This approach is referred to as *free evolution*. A different approach, which we shall adopt in the second part of this thesis, is *constrained evolution*, whereby the constraints (11) and (12) are solved explicitly in lieu of some of the evolution equations. This will give us better control of the asymptotic behaviour of the fields; constrained evolution schemes are also often found to be more stable in highly nonlinear gravitational collapse simulations. Of course the constraints add to the number of elliptic equations to be solved at each time step.

#### 1.4. Numerical methods

Once we have decided on a particular formulation of the Einstein equations, the question arises which numerical methods should be used to solve this system of PDEs. Here we briefly review the two methods that are most often used in numerical relativity: pseudo-spectral methods and finite-difference methods. These methods work well for smooth solutions, which is the case for the vacuum Einstein equations and also for most radiative forms of matter (e.g., scalar, electromagnetic or Yang-Mills fields). For matter that may form discontinuities, e.g. perfect fluids, these methods are generally not suitable. In this case finite-volume methods are normally used for the matter evolution equations.

*1.4.1. Pseudo-spectral methods* The basic idea of spectral methods is an expansion of the numerical approximation  $u(x)$  in a known set of basis functions  $u_n(x)$ , here in one dimension for simplicity:

$$u(x) = \sum_{n=0}^N a_n u_n(x). \quad (14)$$

The  $u_n(x)$  usually belong to a complete orthonormal set of functions. In the spherical topology that is most often encountered in numerical relativity, one usually expands in Chebyshev polynomials in the radial direction and spherical harmonics in the angular directions. Hereby the radial direction is often divided into a few subdomains and an expansion of the form (14) is used in each of the subdomains.

Derivatives of  $u(x)$  can be computed *exactly* within the approximation (14) using the known derivatives of the basis functions. In order to compute nonlinear terms, *pseudo-spectral* methods evaluate the approximation  $u(x)$  at a discrete set of collocation points  $x_i$ , usually the Gauss- or Gauss-Lobatto points of the numerical quadrature associated with the basis functions. Nonlinear terms are evaluated at these collocation points and thereafter the spectral expansion coefficients  $a_n$  of the result are computed.

<sup>+</sup> The constraints always need to be solved at the initial time.



For smooth solutions, pseudo-spectral methods converge exponentially with the number  $N$  of expansion coefficients. Hence  $N$  is usually taken to be quite small,  $N \lesssim 50$ . For larger  $N$  roundoff errors quickly spoil any further gain in accuracy.

*1.4.2. Finite-difference methods* Finite-difference methods are based on an expansion of the solution in a (finite) Taylor series. Derivatives are replaced with difference quotients, e.g. for a one-dimensional uniform grid with spacing  $h$ :

$$(u')_i = \frac{1}{2h}(u_{i+1} - u_{i-1}) + O(h^2), \quad (15)$$

where  $u_i := u(x_i)$ . Near a boundary, one-sided operators are often used, e.g. for a right boundary at  $x = x_N$ :

$$(u')_N = \frac{1}{2h}(3u_N - 4u_{N-1} + u_{N-2}) + O(h^2). \quad (16)$$

The above are examples of second-order accurate finite difference operators; in the second part of this thesis we will work with fourth-order accurate finite differences.

A subtle point is the treatment of coordinate singularities, e.g. for axisymmetric spacetimes on the axis of symmetry  $\rho = 0$  in cylindrical polar coordinates  $\rho, z, \phi$ . For this we use a staggered grid, where the first grid point is at  $x_1 = h/2$ , and we add a *ghost point* at  $x_0 = -h/2$ . (One ghost point suffices for second-order accurate finite differences; two are needed for fourth-order accuracy.) The evolved fields are either even or odd with respect to  $\rho$ . For an even function  $u$  we set  $u_0 = u_1$ , whereas for an odd function we set  $u_0 = -u_1$ . This allows us to use centred finite difference operators at all interior points  $i \geq 1$ .

*1.4.3. Multigrid for elliptic equations* For the constrained evolution schemes considered in the second part of this thesis, elliptic equations need to be solved at each time step and hence an efficient elliptic solver is needed. The matrices arising from finite-difference approximations to elliptic equations are sparse. Standard relaxation method such as Gauss-Seidel relaxation are efficient in damping short-wavelength components of the numerical error. The slow convergence for longer wavelengths can be accelerated by using a hierarchy of grids with increasingly coarser grid spacings, between which the numerical approximation is transferred: the multigrid method ([28]; an excellent concise introduction is [29]). We use the Full Approximation Storage variant of the algorithm in order to treat nonlinearities in the equations directly, combined with a nonlinear Gauss-Seidel relaxation.

*1.4.4. Time integration* A framework often used in numerical relativity is the method of lines: the equations are first discretised in space and then regarded as a large system of ordinary differential equations (ODEs) in time, one at each grid/collocation point. Standard ODE methods (e.g. Runge-Kutta) can be used to integrate these ODEs forward in time.

Some care must be taken in order to insure stability of the method, in addition to the usual Courant-Friedrichs-Lewy condition on the timestep. Finite-difference methods typically require artificial Kreiss-Oliger [30, 31] dissipation for stability in the context of the method of lines. It is important to note though that these extra terms are below the level of the truncation error. Pseudo-spectral methods often suffer from aliasing arising from the pointwise evaluation of nonlinear terms. This can be cured by some form of spectral filtering [32]. An example is Orszag's Two-Thirds rule, whereby the upper third of the expansion coefficients is set to zero prior to evaluation of nonlinear terms.

## 2. The outer boundary problem for isolated systems

A common task one faces in numerical relativity is the modelling of an *isolated system*, i.e. a compact self-gravitating object, e.g. a star, surrounded by an asymptotically flat spacetime. Here asymptotically flat means in a very loose sense that the spacetime metric approaches the Minkowski metric in the limit of infinite distance from the source. It should be stressed that this picture is an idealisation: of course the universe is full of compact objects, and whether the universe is asymptotically flat is a matter of debate. Nevertheless, if we are only interested in the dominant contribution of one particular distant object to, say, the gravitational radiation observed on the earth, then it is often a good approximation to surround this object by an asymptotically flat vacuum spacetime and to consider ourselves to be at infinite distance from the source. The problem then arises to model an asymptotically flat spacetime of infinite extent with finite computational resources, and this is the main subject of this thesis.

### 2.1. Conformal infinity

In order to illustrate the various approaches to this problem, it is convenient to adopt Penrose's idea of *conformal compactification* [33]. We write the spacetime metric as a conformal factor times a conformally related metric:

$$g_{ab} = \Omega^{-2} \tilde{g}_{ab}. \quad (17)$$

Now we map the spacetime coordinates to a compact region such that  $\Omega$  vanishes at the boundary, and  $\tilde{g}_{ab}$  is everywhere finite when evaluated in components with respect to the compactified coordinates.

As an example, consider Minkowski spacetime

$$g = -dt^2 + dr^2 + r^2 \sigma, \quad (18)$$

where  $\sigma := d\theta^2 + \sin^2 \theta d\phi^2$  is the round metric on the unit sphere. Performing the coordinate transformations

$$u = t - r, \quad v = t + r, \quad p = \arctan u, \quad q = \arctan v, \quad T = p + q, \quad R = q - p, \quad (19)$$

the metric can be written in the form (17) with

$$\Omega = 2 \cos p \cos q, \quad \tilde{g} = -dT^2 + dR^2 + (\sin^2 R) \sigma. \quad (20)$$

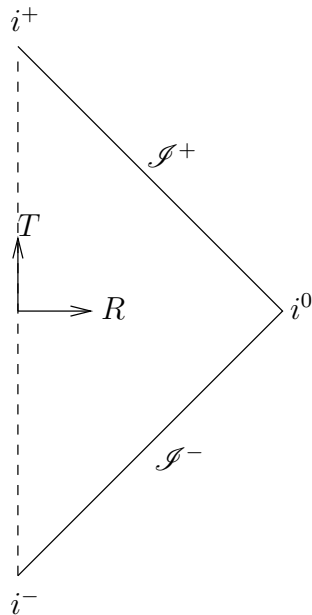


**Figure 2.** Penrose diagram of Minkowski spacetime.

Hence Minkowski spacetime is conformally related to the manifold  $\mathbb{R} \times S^3$  with standard metric. However we obtain only part of this “Einstein cylinder”: the ranges of the compactified coordinates are

$$-\frac{\pi}{2} < p \leq q < \frac{\pi}{2} \quad \Rightarrow \quad -\pi < T < \pi, \quad 0 \leq R < \pi, \quad T + R < \pi, \quad T - R > -\pi. \quad (21)$$

The resulting *Penrose diagram* is shown in figure 2. Since the mapping is conformal, light rays, i.e. null geodesics, propagate at 45 degrees in the  $T, R$  plane, just as they did in the original  $t, r$  coordinates. An analysis of the asymptotic behaviour of geodesics leads to the following results. Future-directed timelike geodesics approach the point  $(T, R) = (\pi, 0)$ , which is therefore called *future timelike infinity*  $i^+$ . Similarly, past-directed timelike geodesics approach  $(T, R) = (-\pi, 0)$ , *past timelike infinity*  $i^-$ . Future-directed null geodesics approach the surface  $T + R = \pi$ , *future null infinity*  $\mathcal{I}^+$  (“Scri+”). Past-directed null geodesics approach  $T - R = -\pi$ , *past null infinity*  $\mathcal{I}^-$ . Finally, spacelike geodesics approach  $(T, R) = (0, \pi)$ , *spacelike infinity*  $i^0$ . Note that the conformal factor  $\Omega$  in (20) vanishes at  $\mathcal{I}^\pm$ . We refer the reader to [34] for an in-depth discussion of conformal infinity.

Similar Penrose diagrams can be drawn for other spacetimes. New features can arise, e.g. singularities and event horizons in black hole spacetimes. For our purposes at this point, we are mainly interested in the asymptotic region, in particular spacelike infinity and null infinity, which is common to all asymptotically flat spacetimes. Hence Minkowski spacetime will serve us as a representative example of an asymptotically flat spacetime.

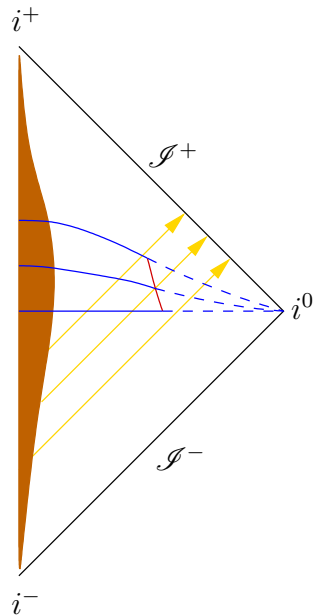


**Figure 3.** Cauchy evolution (blue lines) with artificial timelike boundary (red line). Shown is the Penrose diagram of Minkowski spacetime with a source (brown region) of radiation (yellow arrows).

## 2.2. Initial-boundary evolution

The standard method for numerical evolutions of asymptotically flat spacetimes is to foliate spacetime by spacelike hypersurfaces all approaching spacelike infinity, drawn in blue in figure 3, with initial data specified on an initial slice. Consider a sequence of signals propagating at the speed of light, symbolised by the diagonal yellow lines in figure 3. Since all spatial slices approach  $i^0$ , these signals can never leave the slices. Suppose we wanted to compactify the slices by mapping  $i^0$  to a finite spatial coordinate location. Then an outgoing wave would appear increasingly “blue-shifted” (i.e. with decreasing wavelength) with respect to the compactified coordinates, and would ultimately fail to be resolved on the numerical grid. Thus compactifying towards spacelike infinity is normally not a good idea. (In [2] we assess the numerical performance of this approach, among others.)

For these reasons one usually truncates the spatial slices at a finite distance. This introduces an artificial timelike boundary, the red line in figure 3. Boundary conditions must be imposed there so as to obtain a well-posed initial-boundary value problem. These boundary conditions are not arbitrary because the constraint equations must hold on each individual slice. Furthermore, ideally one would like the solution on the truncated domain to be identical with the solution on the unbounded domain. Spurious reflections of gravitational radiation should be avoided. Such boundary conditions are called *transparent* or *absorbing*. The first part of this thesis will be devoted to the analysis and numerical implementation of these questions, and will be summarised in section 3 below. For a comprehensive review article of this field of research see [35].

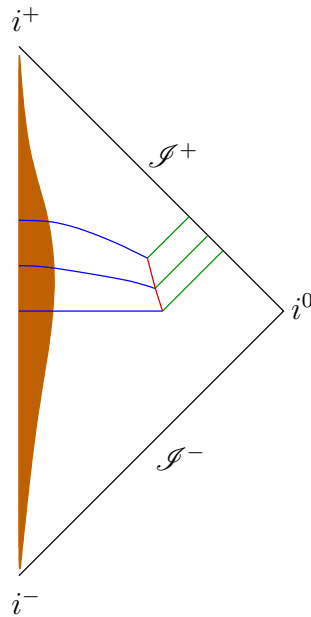


**Figure 4.** Cauchy-characteristic matching. An inner Cauchy foliation (blue) is matched to an outer characteristic foliation (green).

There is a fundamental problem with this approach: in general relativity, gravitational radiation is only well defined at future null infinity  $\mathcal{I}^+$ . This is the result of the seminal work by Bondi, Sachs and coworkers in a series of papers from the 1960s [36]. At a finite distance a “local flux of gravitational radiation” cannot be defined in the full nonlinear theory. This is only meaningful if one linearises about a given background spacetime, e.g. Minkowski or more generally, Schwarzschild or Kerr spacetime. Any absorbing boundary conditions imposed at a finite distance can therefore only be approximate.

### 2.3. Cauchy-perturbative and Cauchy-characteristic matching

One approach is to match the fully nonlinear evolution in the interior to an outer module that solves the *linearised* Einstein equations. Gauge-invariant treatments of gravitational perturbations exist that require the solution of a scalar master equation, one for each pair  $(\ell, m)$  with respect to a spherical harmonic expansion of the gravitational field. These scalars are functions of  $t$  and  $r$  only so it is relatively inexpensive computationally to move the outer boundary to a very large distance. Some more details of this method are discussed in section 3.3. It should be stressed that the linearised equations are still solved on Cauchy slices approaching spacelike infinity  $i^0$ .

A different approach is to attach to the truncated spacelike foliation a *characteristic* foliation extending to future null infinity  $\mathcal{I}^+$ . This is represented by the green lines in figure 4. The “blue-shift problem” mentioned above does not apply to these null slices and hence it is straightforward to compactify them. The difficult part of this method is the matching that needs to be done at the artificial boundary. So far this has been

successfully implemented for *a posteriori* characteristic extraction, whereby one first carries out a Cauchy evolution with boundary and then, in a post-processing step, reads out boundary data for the subsequent characteristic evolution. For this to work reliably, one needs to make sure that the artificial boundary is placed sufficiently far out so that any inaccuracies emanating from it do not reach the extraction surface, which is rather wasteful. So far the ultimate task of doing the matching “on the fly” while the Cauchy evolution is still running has not been fully accomplished. We refer to [17] for a review of the Cauchy-characteristic matching approach.

The reader might wonder why one does not get rid of the spatial foliation altogether and extend the characteristic slices all the way to the centre. The reason is that null geodesic congruences, to which these slices are tied, are generally ill behaved in strong-field regions: they tend to form *caustics*, which lead to coordinate singularities. This caveat does not apply to situations with a high degree of symmetry, e.g. spherical symmetry, where characteristic evolution has indeed been successfully used since the early days of numerical relativity.

#### 2.4. Hyperboloidal evolution

Yet another approach, taken in the second part of this thesis, is to foliate spacetime by *hyperboloidal* surfaces (figure 5). These are spacelike but approach future null infinity rather than spacelike infinity. An example are the standard hyperboloids in Minkowski spacetime,

$$t = \sqrt{r^2 + \left(\frac{3}{K}\right)^2}, \quad (22)$$

where the constant  $K$  turns out to be the mean curvature of the slices. Such constant mean curvature surfaces can be constructed in more general spacetimes, and will be used in the second part of this thesis. However other choices of hyperboloidal surfaces are possible.

The hyperboloidal initial value problem consists in specifying initial data on an initial hyperboloidal surface and evolving them to the future. Note that hyperboloidal surfaces are only partial (future) Cauchy surfaces.

We will follow Penrose’s idea and work with a conformally related metric in a compactified coordinate system. Unfortunately, the Einstein equations as such are not conformally invariant, and as a result develop terms that are formally singular at  $\mathcal{I}^+$ . Dealing with these terms is the main challenge in [4].

### 3. Cauchy evolution with artificial timelike boundary

This section summarises my work on initial-boundary value problems for the Einstein equations, represented by the three papers [1]–[3] in the first part of this thesis.

My interest in this topic arose during my time as a postdoc in the Caltech group, who had just developed a first-order reduction [21] of the generalised harmonic

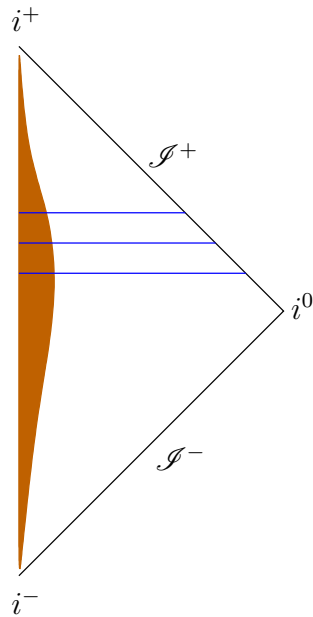


**Figure 5.** Hyperboloidal evolution.

formulation of the Einstein equations (section 1.3.1). They had proposed on physical grounds a set of boundary conditions that seemed to work well in numerical simulations, and they were now interested in proving that these boundary conditions actually rendered the initial-boundary value problem well posed.

### 3.1. Well posedness [1]

The generalised harmonic formulation is convenient from a mathematical point of view because it is essentially a system of nonlinear wave equations, and the initial-boundary value problem for such equations is relatively well understood. However several complications arise in the Einstein case.

For simplicity, let us consider the scalar wave equation (with a source  $F$ ),

$$u_{tt} = u_{xx} + u_{yy} + u_{zz} + F \quad (23)$$

on the half-space

$$x \geq 0, \quad -\infty < y < \infty, \quad -\infty < z < \infty \quad (24)$$

with boundary conditions

$$\alpha u_t = u_x + \beta_1 u_y + \beta_2 u_z + \alpha q \quad \text{at } x = 0, \quad (25)$$

where  $\alpha > 0$  is a constant and  $q$  are boundary data. The initial data are

$$u = f_1, \quad u_t = f_2 \quad \text{at } t = 0. \quad (26)$$

One should think of  $u$  as representing the individual components of the metric in the generalised harmonic formulation of the Einstein equations.

For  $\beta_1 = \beta_2 = 0$  the boundary conditions are maximally dissipative. Defining the energy

$$E := \|u_t\|^2 + \|u_x\|^2 + \|u_y\|^2 + \|u_z\|^2, \quad (27)$$

it is straightforward to obtain an estimate of the form

$$\int_0^t \|\mathbf{u}(s)\|^2 ds + \int_0^t \|\mathbf{u}(s)\|_B^2 ds \leq K_T \left( \|\mathbf{f}\|^2 + \int_0^t \|F(s)\|^2 ds + \int_0^t \|q(s)\|_B^2 ds \right) \quad (28)$$

for every finite time interval  $0 \leq t \leq T$  with a constant  $K_T$  that is independent of  $F$ ,  $f_1$ ,  $f_2$  and  $q$ . Here  $\|\cdot\|$  and  $\|\cdot\|_B$  denote the  $L_2$  norms over the half-space and boundary, respectively, and we have defined the vectors  $\mathbf{u} := (u, u_t, u_x, u_y, u_z)$  and  $\mathbf{f} := (f_1, f_2, f_{1x}, f_{1y}, f_{1z})$ . The initial-boundary value problem is said to be *strongly well posed*.

As already mentioned in section 2.2, boundary conditions for Einstein's equations must be compatible with the constraint equations on the  $t = \text{const}$  hypersurfaces. The constraints satisfy a nonlinear wave equation of their own (6). The simplest constraint-preserving boundary condition one could imagine is

$$\mathcal{C}_a \stackrel{\wedge}{=} 0, \quad (29)$$

where  $\stackrel{\wedge}{=}$  denotes equality at the boundary. This condition is of first order w.r.t. derivatives of the metric, i.e. of the form (25), but unfortunately with  $\beta_1, \beta_2 \neq 0$ , i.e. not maximally dissipative. Later Kreiss and collaborators managed to prove strong well posedness for a set of boundary conditions including (29) using energy methods with a non-standard choice of energy norm [37].

Still, the boundary conditions (25) are too restrictive in many respects. The constraint-preserving boundary conditions (29) are a Dirichlet condition for a wave equation (6). Consequently, any constraint violations generated in the interior will be reflected off the boundary. Better behaved boundary conditions can be obtained by requiring the incoming characteristic fields of (6) to vanish at the boundary so that the constraint violations will leave the domain. However, this will involve first derivatives of the  $\mathcal{C}_a$  and hence second derivatives of the metric. More seriously, absorbing boundary conditions will also involve second (or higher) derivatives of the metric. This is because gravitational radiation is encoded in the Weyl tensor  $C_{abcd}$  (the tracefree part of the Riemann curvature tensor), which contains second derivatives of the metric. In [1] we use as a ‘‘physical’’ boundary condition the vanishing of a particular projection of the Weyl tensor, the Newman-Penrose scalar

$$\Psi_0 = -C_{abcd} l^a m^b l^c m^d. \quad (30)$$

Here the vectors on the right-hand side are part of a Newman-Penrose tetrad  $(l^a, k^a, m^a, \bar{m}^a)$ , where  $l^a$  and  $k^a$  are outgoing and ingoing real null vectors satisfying  $l^a k_a = -1$ ,  $m^a$  is a complex spatial null vector orthogonal to  $l^a$  and  $k^a$ , and  $\bar{m}^a$  is its complex conjugate, with  $m^a \bar{m}_a = 1$ .  $\Psi_0$  can be regarded as an approximation to the incoming gravitational radiation.



For boundary conditions of higher derivative order than (25), the energy method can no longer be applied. Instead, pseudo-differential techniques can be used. For the time being we assume the source terms  $F$  and initial data  $f_1, f_2$  vanish. The idea is to perform a Fourier-Laplace transform and write the solution as a superposition of modes

$$u(t, x, y, z) = \tilde{u}(x) \exp[st + i(\omega_y y + \omega_z z)] \quad (31)$$

with  $s \in \mathbb{C}$  and  $\omega_y, \omega_z \in \mathbb{R}$ . Suppose the homogeneous problem with vanishing boundary data ( $q = 0$ ) admits a solution with  $\text{Re } s > 0$ . Then we obtain another solution by multiplying the exponent in (31) with any real number. Hence the initial-boundary value problem cannot be well posed because the growth of the solution cannot be controlled.

As reviewed in [1], this condition amounts to showing that a certain complex determinant does not have any zeros  $s$  with  $\text{Re } s > 0$ , the *determinant condition*. What remains to be shown is that for the inhomogeneous problem, the solution can be bounded in terms of the boundary data. This turns out to be possible only if the zeros of the determinant have strictly negative real part, the *Kreiss condition*. If it holds then one obtains an estimate

$$\int_0^t \|\mathbf{u}(s)\|^2 ds \leq K_T \int_0^t \|q(s)\|_B^2 ds \quad (32)$$

and the system is said to be *boundary stable*. The main result of [1] is that this condition holds for the given first-order reduction of the generalised harmonic Einstein equations and the given boundary conditions.

A stronger estimate that includes the source terms  $F$  on the right-hand side (cf. (28)) is referred to as *strong well posedness in the generalised sense*. In addition to boundary stability this requires the construction of a symmetriser [38]. For the first-order reduction of the generalised harmonic Einstein equations used in [1] it was not clear how to construct such a symmetriser. What we do show though is that the Kreiss condition rules out so-called weak instabilities with polynomial time dependence.

Later in [39] strong well posedness in the generalised sense was proved for the original second-order form of the equations, avoiding complications arising from the first-order reduction. From the theory of pseudo-differential operators it follows that strong well posedness in the generalised sense carries over to systems with variable coefficients and quasi-linear systems such as the Einstein equations.

Lacking a full proof of strong well posedness, we perform numerical experiments in order to probe the stability of the system. The numerical implementation uses pseudo-spectral methods as described in section 1.4.1. The boundary conditions are implemented via a projection method, which modifies the evolution equations at the boundary by eliminating (derivatives of) the incoming fields using the boundary conditions.

We perform *robust stability tests*, whereby small random noise is injected in the initial data and source terms. The background solution is taken to be either Minkowski spacetime on a spatial domain with topology  $T^2 \times \mathbb{R}$  or Schwarzschild spacetime on  $S^2 \times \mathbb{R}$ . These experiments show no signs of instabilities and strongly support the claim

that the system is well posed. The expected instability for a deliberately chosen set of ill-posed boundary conditions is also reproduced.

### 3.2. Numerical comparisons [2]

Having constructed a set of stable (and most likely well-posed) boundary conditions for the Einstein equations in generalised harmonic gauge, the question arises how well these boundary conditions perform numerically compared to other choices. Perfect boundary conditions would produce a solution on the truncated domain that agrees with the solution on the unbounded domain restricted to the truncated region. We can use this principle in order to assess the boundary conditions in the following way. First we compute a *reference solution* on a very large domain. Because of the finite speed of propagation for hyperbolic PDEs, we can choose the boundary to be sufficiently far out so that any inaccuracies emanating from it remain out of causal contact with the interior region where comparisons will be made. Next we perform an evolution with the same initial data on a domain that is truncated at a much smaller distance, where the boundary conditions are imposed that are to be assessed. Finally we compare the solution on the truncated domain with the reference solution.

The test problem chosen in [2] is a Schwarzschild black hole with an outgoing gravitational wave perturbation. The background spacetime is written in Kerr-Schild coordinates, which penetrate the event horizon at  $r = 2M$ . We can remove the interior of the black hole from the computational domain by placing an *excision* boundary just inside the event horizon. At this interior boundary all characteristics leave the domain so that no boundary conditions are required. The gravitational wave perturbation is taken to be an exact solution of the linearised (about flat space) Einstein equations with quadrupolar ( $\ell = 2$ ) angular dependence [40]. The wave is taken to be outgoing initially, with a Gaussian profile. Of course the constraints must be solved in order to obtain a valid set of initial data for the Einstein equations.

The numerical implementation uses the same pseudo-spectral methods as in [1] and as described above in section 1.4.1.

Once the wave reaches the outer boundary, the imperfect boundary conditions will generate reflections, which propagate into the interior. In order to assess the amount of reflections, we evaluate the following quantities.

- (i) The difference  $\Delta\mathcal{U}$  between the test solution and the reference solution of all components of the metric and their first derivatives, in a suitable norm (see [2] for details). It should be stressed that  $\Delta\mathcal{U}$  is coordinate dependent so it will measure how well the solutions agree *in the given coordinates*. While “gauge reflections” have no physical meaning, they do matter from a numerical point of view as one does not want to waste resolution on short-wavelength features that merely correspond to a coordinate transformation.
- (ii) Violations of the constraints  $\mathcal{C}$ , again in a suitable norm. This quantity tests how well the boundary conditions preserve the constraints.

- (iii) The difference between the test solution and the reference solution of the outgoing gravitational radiation as measured by the Newman-Penrose scalar (cf. (30))

$$\Psi_4 = -C_{abcd}k^a\bar{m}^bk^c\bar{m}^d. \quad (33)$$

This quantity is computed on a sphere close to the outer boundary of the truncated domain (a procedure often referred to as *wave extraction*) and compared to the reference resolution. From a physical point of view it is important to understand how the accuracy of the extracted waveform is affected by the choice of boundary conditions.

The benchmark set of boundary conditions used in [2] are the boundary conditions constructed and analysed in [1], with one small modification: for the components of the metric that can be loosely identified as the “gauge degrees of freedom”, a slightly different boundary condition is used that differs from the original one only in a lower-order term. With this extra term the gauge boundary condition is exactly absorbing for a spherical ( $\ell = 0$ ) gauge wave. This small modification is found to lead to a substantial reduction of the coordinate-dependent difference  $\Delta\mathcal{U}$ , whereas the constraints  $\mathcal{C}$  and physical radiation  $\Delta\Psi_4$  are of course unaffected.

In the following we summarise the various alternate boundary conditions that are investigated in [2], along with their numerical performance.

- (i) *Freezing the incoming fields.* In this approach the time derivatives of all the incoming fields are required to vanish at the outer boundary. While these boundary conditions render the initial-boundary problem well posed, they are neither constraint preserving nor absorbing. For increasing numerical resolution the quantity  $\mathcal{C}$  is seen to converge to a nonzero function. This demonstrates that one does in fact not obtain a solution to Einstein’s equations with these simple-minded boundary conditions.
- (ii) *Sommerfeld boundary conditions.* This type of condition is often used in numerical relativity simulations based on the BSSN system and corresponds to imposing

$$(\partial_r + \partial_t + r^{-1})(g_{ab} - \eta_{ab}) \stackrel{\wedge}{=} 0 \quad (34)$$

on all components of the metric at the outer boundary, where  $\eta_{ab}$  is the flat (Minkowski) metric. The numerical performance is similar to the boundary conditions described above, with slightly reduced constraint violations.

- (iii) *Kreiss-Winicour boundary conditions.* These conditions, proposed in [38], consist in requiring the harmonic constraints to vanish at the boundary, equation (29) above. We compute the remaining incoming characteristic fields from the Schwarzschild background solution. Although we expected this condition to be more reflective for constraint violations, we do not find any indications for this numerically. Apparently the constraint damping terms in our formulation are very effective in reducing any constraint violations before they reach the boundary. However we do see larger errors in the physical quantities  $\Psi_4$  than with our benchmark boundary conditions, which include the condition  $\Psi_0 \stackrel{\wedge}{=} 0$ .

- (iv) *Spatial compactification.* This approach is not technically a boundary condition; instead we compactify the spatial domain towards spatial infinity (see the discussion at the beginning of section 2.2 above). A certain form of spectral filtering is applied in order to damp the outgoing waves as they become increasingly “blue-shifted”. This turns out to work quite well as far as constraint violations are concerned, however the errors in  $\Psi_4$  are significantly larger than with our benchmark boundary conditions.
- (v) *Sponge layers.* This method, often used in the context of spectral methods, adds artificial damping terms to the evolution equations that are only active in a region close to the outer boundary, schematically:

$$\partial_t u = \dots - \gamma(r)(u - u_0), \quad (35)$$

where  $u_0$  refers to the background solution and the function  $\gamma(r)$  is non-negligible only close to the outer boundary. This method is found to lead to a small amount of constraint violations and to considerable errors in the outgoing radiation  $\Psi_4$ .

In summary, our boundary conditions outperform all the alternate methods considered here. We can even compare the reflection coefficient  $\Psi_0/\Psi_4$  with the prediction from linearised theory and find good agreement with our simulations.

### 3.3. Absorbing boundary conditions [3]

The boundary conditions used in [1, 2] included a condition on the vanishing of the Newman-Penrose scalar  $\Psi_0$ , which can be regarded as an approximation to the outgoing gravitational radiation. Using this condition was found to significantly reduce spurious reflections of gravitational radiation. It turns out that one can do better: there is a hierarchy of absorbing boundary conditions of the form

$$[r^2(\partial_t + \partial_r)]^{L-1}(r^5\Psi_0) \stackrel{\wedge}{=} 0. \quad (36)$$

Here  $L$  refers to an expansion of the gravitational field in spherical harmonics. The boundary condition (36) is perfectly absorbing for linearised gravitational waves on a flat background spacetimes for all spherical harmonic modes  $\ell \leq L$ . For  $L = 1$  we recover our original condition  $\Psi_0 \stackrel{\wedge}{=} 0$ .

The boundary conditions (36) were first suggested by Buchman and Sarbach [41]. They considered the linearised Bianchi equations, which describe the propagation of gravitational radiation and in vacuum take the form

$$\nabla^a C_{abcd} = 0, \quad (37)$$

where  $C_{abcd}$  is the Weyl tensor. By expanding the fields in spherical harmonics and constructing exact solutions to the linearised equations, the conditions (36) were designed to eliminate the ingoing solutions. Later Buchman and Sarbach generalised their method to a Schwarzschild background [42].

In [3] we reformulate the boundary conditions in a way that is both conceptually more straightforward and more amenable to numerical implementation. Gravitational

perturbations can be described by the gauge-invariant Regge-Wheeler-Zerilli (RWZ) scalars  $\Phi_{\ell m}^{(\pm)}$  (see [43] and references therein). These are complex quantities, one for each spherical harmonic index  $(\ell, m)$  and for two parities: even (+) and odd (-). On a flat background, they obey the master equation

$$\left[ \partial_t^2 - \partial_r^2 + \frac{\ell(\ell+1)}{r^2} \right] \Phi_{\ell m}^{(\pm)} = 0. \quad (38)$$

This equation is known as the Euler-Poisson-Darboux equation; it is of course just the scalar wave equation in disguise. The general outgoing and ingoing solutions have the form

$$\Phi_{\ell m}^{(\pm)\text{out}}(t, r) = \sum_{j=0}^{\ell} \frac{f_{j\ell m}^{(\pm)}(t-r)}{r^j}, \quad \Phi_{\ell m}^{(\pm)\text{in}}(t, r) = \sum_{j=0}^{\ell} \frac{g_{j\ell m}^{(\pm)}(t+r)}{r^j}. \quad (39)$$

The precise form of the functions  $f_{j\ell m}^{(\pm)}$  and  $g_{j\ell m}^{(\pm)}$  does not matter here. The key observation is that

$$B_L \Phi_{\ell m}^{(\pm)\text{out}} := [r^2(\partial_t + \partial_r)]^{L+1} \Phi_{\ell m}^{(\pm)\text{out}} = 0 \quad (40)$$

provided that  $L \geq \ell$ . Using  $B_L \Phi_{\ell m}^{(\pm)} \stackrel{\wedge}{=} 0$  as a boundary condition will therefore eliminate the ingoing solutions for all  $\ell \leq L$ . These are nothing but the well-known boundary conditions of Bayliss and Turkel [44] for the scalar wave equation. It is straightforward to relate them to conditions on the Newman-Penrose scalar  $\Psi_0$  and recover (36).

Equation (40) contains higher derivatives, which are difficult to treat numerically. In [3] we address this by introducing a set of auxiliary variables so that (40) can be written as a system of ODEs intrinsic to the boundary.

So far we have only considered the RWZ equation (38). What we would really like is a set of boundary conditions for the Einstein equations, in the generalised harmonic formulation already used in the previous work. Our algorithm thus consists in three steps:

- (i) extraction of the RWZ scalars from the spacetime metric at the boundary,
- (ii) evolution of the system of ODEs for the auxiliary variables that implements the desired absorbing boundary condition,
- (iii) construction of boundary data for certain incoming characteristic fields of the Einstein equations from the auxiliary variables.

In [3] we describe each of these steps in detail.

Step (iii) can also be used as a recipe for Cauchy-perturbative matching (section 2.3) in the context of the generalised harmonic formulation of the Einstein equations, as we could equally well take the boundary data from an outer module that evolves the RWZ equations directly.

We also remark that strong well posedness in the generalised sense (see section 3) was proved in [39] for the original second-order form of the Einstein equations in harmonic gauge with the new higher-order absorbing boundary conditions as well.

From the numerical point of view, an expansion of the fields in spherical harmonics is required. This fits well with our pseudo-spectral method, which already uses spherical harmonics as the angular basis functions. However some slightly intricate transformations between different representations of tensor spherical harmonics need to be carried out (see the appendix of [3]).

In order to test our numerical implementation, we evolve initial data corresponding to outgoing solutions of the linearised Einstein equations with fixed spherical harmonic dependence  $(\ell, m)$ . For  $\ell = 2$  these were derived in [40]. In [45] I constructed analogous solutions for arbitrary  $\ell$ . We evolve these initial data on a truncated spherical domain using our new absorbing boundary conditions. During the evolution we extract the RWZ scalars at the boundary and compare with the analytical solutions. Since we evolve the full nonlinear Einstein equations, whereas the analytical solutions are only valid to linear order, we perform evolutions with different amplitudes of the initial data and check that any quantities that should vanish at the linear level decay (at least) quadratically with amplitude. Using this method we show for our numerical evolutions in [3] that our boundary conditions  $B_L$  are indeed perfectly absorbing for all  $\ell \leq L$ .

While the boundary conditions do not eliminate incoming modes with  $\ell > L$ , they reduce their amplitude significantly. We compute the expected reflection coefficient analytically in linearised theory and find good agreement with our numerical evolutions. For instance, the  $\ell = 3$  incoming mode is suppressed by a factor of about 100 when the  $L = 2$  absorbing boundary condition is used as compared with  $L = 1$ , which corresponds to the old  $\Psi_0 \stackrel{\wedge}{=} 0$  condition\*. This demonstrates the dramatic improvement achieved by these higher-order absorbing boundary conditions.

#### 4. Hyperboloidal evolution to future null infinity

Much progress has been made with initial-boundary value problems for the Einstein equations: well-posed formulations have been derived, particularly in the context of generalised harmonic gauge, and improved absorbing boundary conditions have been constructed and implemented. The fundamental problem remains however that in the full nonlinear theory of general relativity, boundary conditions imposed at a finite distance can never be perfectly transparent in the sense that the solution on the truncated domain agrees with the solution on the unbounded domain. The absorbing boundary conditions considered in [3] rely on the validity of the linear approximation about a given background spacetime (Minkowski in our case).

For this reason I became interested in hyperboloidal evolution, which aims to place the outer boundary of the computational domain at future null infinity  $\mathcal{I}^+$ , the only physically meaningful (conformal) boundary of spacetime. This is the topic of the second part of this thesis [4]–[6].

\* Here we have taken the radius of the outer boundary to be twice the wavelength.

#### 4.1. Regularity at future null infinity [4]

Most approaches to hyperboloidal evolution are based on Penrose's idea of a conformal transformation of the spacetime metric combined with a compactifying coordinate transformation, as described in section 2.1 above. Unfortunately the Ricci tensor is not conformally invariant and as a result the Einstein equations contain inverse powers of the conformal factor, which are singular at  $\mathcal{I}^+$ .

In the early 1980s Friedrich [46] developed an elegant solution to this problem by constructing a symmetric hyperbolic system of PDEs that contained the Einstein equations but also evolution equations for the Weyl curvature. Remarkably, his equations are regular everywhere, including at  $\mathcal{I}^+$ . They are however rather complicated, which may explain why they have not made their way into mainstream numerical relativity, despite a burst of activity in the late 1990s (see [47] for a review). Recently [48] there has been a renewed numerical interest in these equations, especially concerning an extension [49] of Friedrich's original formulation that is able to address the intricate issues that arise where null infinity meets spacelike infinity.

Here we follow a different approach, proposed by Moncrief, that aims to tackle the (formally) singular terms in the Einstein equations directly. We wanted to develop a system that is simpler than Friedrich's regular conformal field equations and more similar to other formulations already used by the numerical relativity community. We work with an ADM-like formulation with elliptic gauge conditions: constant mean curvature slicing and spatially harmonic coordinates, as described in section 1.3.2 above. In the spatially compact case the Cauchy problem for these equations was shown to be well posed [27]; therefore we expect this formulation to be well behaved in our case as well, although a formal proof of well posedness of the hyperboloidal initial value problem with conformal boundary at  $\mathcal{I}^+$  is still lacking.

As expected we find that both the constraints and the evolution equations contain terms involving inverse powers of the conformal factor  $\Omega$ , which become singular at  $\mathcal{I}^+$ . This is not so much of a concern for the constraint equations, as one can always multiply the entire equation by a suitably high power of  $\Omega$  before solving it, but for the evolution equations it seems at first sight that the right-hand sides are singular so that stable evolution near  $\mathcal{I}^+$  cannot be expected. However in [4] we show that the formally singular terms can actually be evaluated explicitly at  $\mathcal{I}^+$  in a completely regular way provided the constraints hold.

On a given hyperboloidal slice, we expand all the fields in finite Taylor series in  $r$  near  $\mathcal{I}^+$ , in adapted coordinates so that  $\mathcal{I}^+$  corresponds to an  $r = \text{const}$  surface. Thanks to the degeneracy of the elliptic constraint equations at  $\mathcal{I}^+$ , we are able to evaluate the first few radial derivatives of the fields at  $\mathcal{I}^+$  by inserting the Taylor expansions into the constraints. More precisely, we obtain the first three radial derivatives of  $\Omega$ , the zeroth and first radial derivative of the components  $\pi^{\text{tr } ri}$  of the ADM momentum (directly related to the tracefree part of the extrinsic curvature), and the first two radial derivatives of the conformal lapse function  $\tilde{\alpha} = \Omega\alpha$ .

With this information we are able to evaluate the formally singular terms in the evolution equation for  $\pi^{\text{tr } ij}$  and show they are regular at  $\mathcal{I}^+$ , subject to one additional condition: the vanishing of the shear of the null geodesic congruence that forms  $\mathcal{I}^+$ . This condition had already been found in [50]. In [4] we show in addition that it is preserved under the time evolution in the sense that if the shear vanishes at one instant of time, then its time derivative vanishes as well.

It is important to note that we only use *finite* Taylor series at  $\mathcal{I}^+$ . We do not assume that the fields are smooth there. The constraint equations give us just enough information about the first few derivatives of the fields at  $\mathcal{I}^+$  so that we can evaluate the formally singular terms in the evolution equations. In fact, it appears that in general, the Taylor expansion already breaks down at the next order and a polylogarithmic term needs to be included [51]. It could be that this is an artefact of CMC slicing. Whether the polylogarithmic terms can be avoided in a different slicing is an interesting open question.

There is a different, more straightforward way of deriving regular evolution equations at  $\mathcal{I}^+$  by assuming that the conformal Weyl tensor vanishes at  $\mathcal{I}^+$ . This *Penrose regularity* implicitly assumes though that the conformal metric is  $C^3$  up to the boundary, a slightly stronger requirement than what we needed for our original analysis. This different regularisation technique is also explored in [4].

#### 4.2. Axisymmetric reduction and numerical implementation [5]

In this section we describe the first successful numerical implementation of the formulation developed in [4]. Since our regularity analysis at  $\mathcal{I}^+$  relied crucially on the satisfaction of the constraint equations, we expect having to solve the constraints explicitly at each timestep (constrained evolution). This is computationally expensive and hence in this first application we assume that spacetime is axisymmetric. This reduces the number of effective spatial dimensions from three to two. Unlike spherical symmetry, it is still compatible with gravitational radiation, and we expect all the difficulties in the non-symmetric case already to be present in axisymmetry as far as numerical stability at  $\mathcal{I}^+$  is concerned. I had already developed a constrained axisymmetric evolution scheme on maximal Cauchy slices with timelike boundary [52, 53] and hence it was obvious to try and adapt it to CMC slices with conformal boundary at  $\mathcal{I}^+$ .

Spherical polar coordinates  $(t, r, \theta, \phi)$  are used so that the Killing vector is  $\partial/\partial\phi$ , which in addition is assumed to be hypersurface orthogonal. The spatial gauge condition used here differs from the spatial harmonic gauge of [4]. The conformal spatial metric  $\tilde{\gamma}_{ij}$ , which is related to the physical spatial metric via  $\gamma_{ij} = \Omega^{-2}\tilde{\gamma}_{ij}$ , is taken to have the form

$$\tilde{\gamma} = e^{2\eta \sin \theta} (dr^2 + r^2 d\theta^2) + r^2 \sin^2 \theta d\phi^2. \quad (41)$$

This is known as *quasi-isotropic gauge* and is chosen here because it reduces the degrees of freedom in the conformal spatial metric to just one function  $\eta(t, r, \theta)$ . Preservation of



this gauge condition in time yields a system of elliptic equations for the shift vector  $\beta^i$ . In addition we need to solve the CMC slicing condition for the conformal lapse  $\tilde{\alpha}$  and the Hamiltonian constraint for the conformal factor  $\Omega$ . There are evolution equations for the function  $\eta$  and for the three components of the tracefree part of the extrinsic curvature.

Even though the spatial gauge condition is different, the regularity analysis at  $\mathcal{I}^+$  carries through as in [4] and we obtain manifestly regular forms of the evolution equations at  $\mathcal{I}^+$ . We have experimented with two slightly different versions, one derived directly from the constraint equations using Taylor expansions, the other by assuming the somewhat stronger Penrose regularity mentioned in the previous subsection. Numerically both appear to work equally well.

The numerical implementation is based on the finite-difference technique (section 1.4.2) with fourth-order accurate finite-difference operators. The outermost radial gridpoint is placed right at  $\mathcal{I}^+$ . Here the regularised versions of the evolution equations are used, with one-sided finite differences. Already one further grid point in we have no choice but to use the full, formally singular evolution equations. Remarkably, this appears to be stable, provided the constraints are solved at each substep of the Runge-Kutta time integration scheme. We provide a heuristic explanation for the success of the method by observing that the evolution equations contain terms that tend to push the solution towards the values dictated by the regularity conditions.

Some care needs to be taken when solving the elliptic equations using multigrid. Since the equations degenerate at  $\mathcal{I}^+$ , it is not surprising that a straightforward pointwise Gauss-Seidel relaxation fails to converge. Instead, we use a radial line relaxation (with a direct one-dimensional solver) and then perform Gauss-Seidel iterations in the angular direction.

As a first test problem we consider a Schwarzschild black hole. The metric on CMC slices is known in closed form; we just need to compactify the radial coordinate, which requires the numerical solution of one ODE. An inner excision boundary is placed just inside the event horizon. We are able to evolve initial data taken from this metric for times  $t \sim 1000M$  ( $M$  being the black hole mass) without any signs of instability and with the expected fourth-order convergence as the numerical resolution is increased.

Next we include a gravitational wave perturbation by specifying free initial data for the function  $\eta$  in (41), which vanishes for the unperturbed Schwarzschild spacetime. We can read out the gravitational radiation at  $\mathcal{I}^+$  by computing the gauge-invariant Bondi news function [36], which can be computed directly from the conformal spacetime Ricci tensor,

$$N = \bar{m}^a \bar{m}^b \tilde{R}_{ab}, \quad (42)$$

where the Newman-Penrose tetrad used must have the property that  $m^a$  is tangential to  $\mathcal{I}^+$ , i.e.  $m^a \partial_a \Omega = 0$ . We observe the expected quasi-normal mode radiation generated by the perturbed black hole (which essentially acts as a damped harmonic oscillator):

$$N_\ell \propto e^{-\kappa_\ell t} \sin(\omega_\ell t + \phi_\ell), \quad (43)$$

where  $\ell$  refers to the index of an expansion in spherical harmonics. For the small perturbation we use ( $\sim 10^{-4}$ ), the values of  $\kappa_\ell$  and  $\omega_\ell$  fitted from our numerical evolution are in good agreement with the semi-analytic results from linear perturbation theory. At later times, when the quasi-normal mode radiation has decayed, one expects a power-law tail (often referred to as *Price's law* [54])

$$N_\ell \propto t^{-p_\ell}. \quad (44)$$

At the numerical resolutions that we are able to afford, we cannot see this tail yet—as runs with two different resolutions demonstrate, the solution has not converged yet. The algorithm will need to be speeded up in order to study these subtle phenomena.

### 4.3. Including matter; numerical evolutions in spherical symmetry [6]

Resolving late-time power-law tails of gravitational and matter fields on black hole backgrounds is a very demanding problem. With the current axisymmetric implementation of our hyperboloidal evolution scheme we were unable to provide sufficiently high resolution. In order to test if our method is capable to study tails in principle, we decided to take one step back and impose spherical symmetry.

Due to Birkhoff's theorem, spherically symmetric vacuum spacetimes are necessarily static: they are isometric to the Schwarzschild solution. Thus in order to have non-trivial dynamics in spherical symmetry, matter needs to be included. How to deal with matter in the context of hyperboloidal evolution based on conformal compactification is an interesting problem in its own right, and so we investigated this quite generally, without any spacetime symmetries at first.

We need to impose the condition that the energy-momentum tensor be tracefree,

$$g^{ab}T_{ab} = 0. \quad (45)$$

Under this assumption the energy-momentum conservation equations, which constitute the evolution equations for the matter fields, are conformally invariant: if we define a conformally related energy-momentum tensor  $\tilde{T}_{ab} := \Omega^{-2}T_{ab}$  then standard energy-momentum conservation  $g^{ab}\nabla_a T_{bc} = 0$  implies that

$$\tilde{g}^{ab}\tilde{\nabla}_a\tilde{T}_{bc} = 0, \quad (46)$$

where  $\tilde{\nabla}$  is the connection compatible with the conformal spacetime metric  $\tilde{g}_{ab}$ . Without the condition (45), the equations (46) contain an additional term that is singular at  $\mathcal{I}^+$ . Condition (45) is generally satisfied for “radiative” forms of matter such as a (conformally coupled) massless scalar field, Maxwell or Yang-Mills fields. It is not satisfied e.g. for a general perfect fluid. However if the support of the matter remains compact during the evolution then one needs not to worry about the singular terms at  $\mathcal{I}^+$ .

We work out the matter evolution equations and matter source terms in the Einstein equations explicitly for two examples: a conformally coupled scalar field and Yang-Mills fields.

The Einstein-scalar field equations arise from varying the action

$$S = \int \left( \frac{1}{2\kappa} R - \frac{1}{2} g^{ab} \phi_{,a} \phi_{,b} - \frac{1}{12} R \phi^2 \right) \sqrt{-g} d^4x. \quad (47)$$

The last term is referred to as *conformal coupling* and leads to a conformally invariant evolution equation for the scalar field  $\phi$ :

$$\square \phi - \frac{1}{6} R \phi = 0 \quad \Leftrightarrow \quad \tilde{\square} \tilde{\phi} - \frac{1}{6} \tilde{R} \tilde{\phi} = 0, \quad (48)$$

where  $\square$  is the d'Alembert operator, as above a tilde refers to the conformal spacetime metric, and we have introduced a rescaled scalar field  $\tilde{\phi} := \Omega^{-1} \phi$ .

Yang-Mills theory can be regarded as a nonlinear generalisation of electromagnetism to non-abelian gauge groups. Its fundamental field is a vector potential or connection  $A_a^{(\alpha)}$ . The upper index refers to the gauge group, which we will take to be  $SU(2)$ , so Greek indices range over 1, 2, 3 here. The associated field strength tensor is

$$F_{ab}^{(\alpha)} = \partial_a A_b^{(\alpha)} - \partial_b A_a^{(\alpha)} + f^{\alpha\beta\gamma} A_a^{(\beta)} A_b^{(\gamma)}. \quad (49)$$

Note the last term, which is absent in electromagnetism. The symbol  $f^{\alpha\beta\gamma} = g[\alpha\beta\gamma]$  is totally antisymmetric, where  $[123] := +1$  and  $g$  is a dimensionful coupling constant. Repeated Greek indices are summed over. The Yang-Mills field equations are given by

$$\nabla_a F^{ab(\alpha)} + f^{\alpha\beta\gamma} A_a^{(\beta)} F^{ab(\gamma)} = 0. \quad (50)$$

They have the convenient property to be conformally invariant and hence we may adorn all quantities in the above equations with tildes and work directly in the conformal spacetime. When performing the 3 + 1 decomposition, the Yang-Mills equations split into a constraint and an evolution equation.

After this general discussion and examples of matter models we reduce the equations to spherical symmetry. Isotropic spatial coordinates are chosen so that the conformal spatial metric is flat. The tracefree part of the extrinsic curvature has only one free component in this case. Unlike in [5], we solve the momentum constraint for it, rather than its formally singular evolution equation. (This is only possible in spherical symmetry.)

While the reduction to spherical symmetry is straightforward for the Einstein and scalar field equations, it is not so obvious for the Yang-Mills fields. The most general spherically symmetric (conformal) Yang-Mills connection has the form

$$\tilde{A}^{i(\alpha)} = [\alpha i j] x^j F + (x^\alpha x^i - r^2 \delta^{\alpha i}) H + \delta^{\alpha i} L, \quad \tilde{A}_0^{(\alpha)} = G x^\alpha, \quad (51)$$

where  $F, H, L$  and  $G$  are functions of  $t$  and  $r$  only. In most previous numerical studies only the potential  $F$  was included; we present for the first time evolutions with fully general spherically symmetric Yang-Mills fields.

Our numerical method is very similar to the one of [5]. Since there is only one spatial dimension now, the constraint equations are ODEs, which we solve using a direct band-diagonal solver combined with an outer Newton-Raphson iteration to address the nonlinearity.

The initial data are chosen to be either Minkowski or Schwarzschild spacetime (in CMC slicing) with an approximately ingoing matter perturbation (scalar field or Yang-Mills). On the flat background we are able to take the amplitude to be large enough so that a black hole forms during the evolution, and to continue the evolution after excising its interior.

With the increased numerical resolution that is possible in the spherically symmetric case, we can now see the tails and measure their decay exponents. The results are in good agreement with previous numerical work. This includes two studies that also used hyperboloidal evolution [55, 56], however in coordinates that are not horizon-penetrating so that gravitational collapse could not be studied.

A general property of power-law tails is that the decay at  $\mathcal{I}^+$  is slower than at a finite distance. (It would be impossible to see this with a code based on Cauchy evolution with artificial timelike boundary!) This causes the solution to resemble a “boundary layer” at late times and the runtime of the simulation at fixed resolution is limited (though sufficient in our case to obtain reliable results).

One feature we find that does not seem to have been noticed before is that in the Yang-Mills case, the electric field (a component of the field strength tensor (49)) has a slower decay rate at  $\mathcal{I}^+$  ( $\sim t^{-1}$ ) than the connection ( $\sim t^{-2}$ ). Furthermore, for the general spherically symmetric connection (51) we find some interesting gauge dynamics: while all components of the energy-momentum tensor decay so that a vacuum solution is approached, the components of the connection approach a constant or even time-periodic solution in some cases. We explain this behaviour by deriving the most general form of the spherically symmetric vacuum solutions to the Einstein-Yang-Mills system.

## 5. Conclusions and outlook

This thesis is concerned with analytical and numerical approaches to treating the far field of asymptotically flat spacetimes satisfying the Einstein equations. We focus on two different approaches: Cauchy evolution with artificial timelike boundary (part 1) and hyperboloidal evolution to future null infinity (part 2).

In the first part, we prove a necessary condition (boundary stability) for well posedness of the initial-boundary value problem for a first-order reduction of the Einstein equations in generalised harmonic gauge with constraint-preserving boundary conditions. These include a condition on the Weyl tensor component  $\Psi_0$ , which can be regarded as a first approximation to the incoming gravitational radiation. Numerical stability tests further demonstrate the robustness of the boundary conditions. Next we assess the numerical performance of various other boundary conditions and alternate approaches such as compactification to spacelike infinity or sponge layers by comparing the solution on the truncated domain with a reference solution on a much larger domain. In all cases our boundary conditions are found to be superior. Finally we formulate and implement a hierarchy of higher-order absorbing boundary conditions that improve on the original  $\Psi_0 \stackrel{\wedge}{=} 0$  condition. Our approach is based on the Regge-Wheeler-Zerilli

scalars, and we show how it can be interfaced with the generalised harmonic formulation of the Einstein equations.

In the second part, we work with a constrained ADM-like formulation of the Einstein equations on constant mean curvature slices extending to future null infinity. Upon a conformal transformation of the metric, the Einstein equations develop terms that are formally singular at future null infinity  $\mathcal{I}^+$ . However, we show explicitly how these terms can be evaluated at  $\mathcal{I}^+$  in a completely regular way. Based on this idea we present a first numerical implementation for vacuum axisymmetric spacetimes. Long-term stable evolutions of a gravitationally perturbed Schwarzschild black hole are obtained and the Bondi news function, which describes the outgoing gravitational radiation in a gauge-invariant way, is evaluated at  $\mathcal{I}^+$ . Finally we extend our formulation to include matter with trace-free energy-momentum tensor. Scalar and Yang-Mills fields are coupled to the Einstein equations and evolved numerically in spherical symmetry. This includes spacetimes that form a black hole from regular initial data. We study the power-law decay (“tail”) of the matter fields at late times, both at  $\mathcal{I}^+$  and at a finite distance.

There are a number of ways in which the research presented in this thesis can be extended. We discuss both parts separately.

Concerning Cauchy evolution with artificial boundary, it would of course be nice to complete the proof of strong well posedness in the generalised sense for the particular first-order reduction of the Einstein equations in generalised harmonic gauge and boundary conditions we used. However, given that there is already a proof for the original second-order system and that the boundary conditions appear to be very robust numerically, there is currently not so much interest in this question. Our implementation of absorbing boundary conditions could be generalised by allowing for a Schwarzschild rather than flat background spacetime. In general however, the numerical relativity community seems to be quite happy with their current codes and seem to be reluctant to invest much effort in improved boundary conditions. This may well change once gravitational wave astronomy has advanced to a stage that even more accurate simulations are required.

Certainly from the current point of view, hyperboloidal evolution appears to be a much cleaner solution to the outer boundary problem. Our axisymmetric numerical implementation demonstrates that stable numerical evolutions based on our approach can be achieved, however the code will need to be speeded up in order to be useful in practice, especially in the case without symmetries. For instance, one could try to solve the constraints explicitly only in a neighbourhood of  $\mathcal{I}^+$  and use free evolution in the interior. We also intend to generalise our formulation to more general gauge conditions, as we do not believe the particular gauge we used (constant mean curvature slicing and spatially harmonic coordinates) was essential for the regularity analysis at  $\mathcal{I}^+$ . Hyperboloidal evolution should have interesting applications whenever global properties of spacetime are to be investigated. An example is cosmic censorship, as one can now check whether null geodesics manage to escape to future null infinity.

## Acknowledgments

I would like to thank my Habilitation committee at FU Berlin (Ralf Kornhuber, Klaus Ecker, Konrad Polthier, Theodora Bourni, Florian Litzinger) and the referees for their time and effort, and for making me welcome at the Department. Further thanks go to my colleagues at the Albert Einstein Institute and my collaborators over the past years who contributed to this work. Support through a Heisenberg Fellowship and grant RI 2246/2 of the German Research Foundation (DFG) is gratefully acknowledged.

## References

- [1] Rinne O 2006 Stable radiation-controlling boundary conditions for the generalized harmonic Einstein equations *Class. Quantum Grav.* **23** 6275–6300 <http://www.arxiv.org/abs/gr-qc/0606053>
- [2] Rinne O, Lindblom L and Scheel M A 2007 Testing outer boundary treatments for the Einstein equations *Class. Quantum Grav.* **24** 4053–4078 <http://www.arxiv.org/abs/0704.0782>
- [3] Rinne O, Buchman L T, Scheel M A and Pfeiffer H P 2009 Implementation of higher-order absorbing boundary conditions for the Einstein equations *Class. Quantum Grav.* **26** 075009 <http://www.arxiv.org/abs/0811.3593>
- [4] Moncrief V and Rinne O 2009 Regularity of the Einstein equations at future null infinity *Class. Quantum Grav.* **26** 125010 <http://www.arxiv.org/abs/0811.4109>
- [5] Rinne O 2010 An axisymmetric evolution code for the Einstein equations on hyperboloidal slices *Class. Quantum Grav.* **27** 035014 <http://www.arxiv.org/abs/0910.0139>
- [6] Rinne O and Moncrief V 2013 Hyperboloidal Einstein-matter evolution and tails for scalar and Yang-Mills fields *Class. Quantum Grav.* **30** 095009 <http://www.arxiv.org/abs/1301.6174>
- [7] Christodoulou D and Klainerman S 1993 *The Global Nonlinear Stability of the Minkowski Space* Mathematical Series (Princeton University Press)
- [8] Penrose R 1969 Gravitational collapse: The role of general relativity *Riv. Nuovo Cimento* **1** 252–276
- [9] Hawking S W and Ellis G F R 1973 *The Large Scale Structure of Space-Time* (Cambridge University Press)
- [10] Hahn S and Lindquist R 1964 The two-body problem in geometrodynamics *Ann. Phys.* **29** 304–331
- [11] Baumgarte T W and Shapiro S L 2010 *Numerical Relativity: Solving Einstein's Equations on the Computer* (Cambridge University Press)
- [12] Alcubierre M 2008 *Introduction to 3+1 Numerical Relativity* International Series of Monographs on Physics (Oxford University Press)
- [13] Choptuik M W 1993 Universality and scaling in gravitational collapse of a massless scalar field *Phys. Rev. Lett.* **70** 9–12
- [14] Pretorius F 2005 Evolution of binary black hole spacetimes *Phys. Rev. Lett.* **95** 121101
- [15] Campanelli M, Lousto C O, Maronetti P and Zlochower Y 2006 Accurate evolutions of orbiting black-hole binaries without excision *Phys. Rev. Lett.* **96** 111101
- [16] Baker J G, Centrella J, Choi D I, Koppitz M and van Meter J 2006 Gravitational wave extraction from an inspiraling configuration of merging black holes *Phys. Rev. Lett.* **96** 111102
- [17] Winicour J 2005 Characteristic evolution and matching *Living Rev. Relativity* **8**(10)
- [18] Cook G B 2005 Initial data for numerical relativity *Living Rev. Relativity* **3**(5)
- [19] Fourès-Bruhat Y 1952 Théorème d'existence pour certains systèmes d'équations aux dérivées partielles non linéaires *Acta Math.* **88** 141–225
- [20] Gundlach C, Calabrese G, Hinder I and Martín-García J M 2005 Constraint damping in the Z4 formulation and harmonic gauge *Class. Quantum Grav.* **22** 3767–3774

- [21] Lindblom L, Scheel M A, Kidder L E, Owen R and Rinne O 2006 A new generalized harmonic evolution system *Class. Quantum Grav.* **16** S447–S462
- [22] Arnowitt R, Deser S and Misner C W 1962 The dynamics of general relativity *Gravitation: An Introduction to Current Research* ed Witten L (New York: Wiley) chap 7
- [23] York Jr J W 1979 Kinematics and dynamics of general relativity *Sources of Gravitational Radiation* ed Smarr L L (Cambridge University Press) pp 83–126
- [24] Reula O 1998 Hyperbolic methods for Einstein’s equations *Living Rev. Relativity* **1**(3)
- [25] Shibata M and Nakamura T 1995 Evolution of three-dimensional gravitational waves: Harmonic slicing case *Phys. Rev. D* **52** 5428
- [26] Baumgarte T W and Shapiro S L 1998 Numerical integration of Einstein’s field equations *Phys. Rev. D* **59** 024007
- [27] Andersson L and Moncrief V 2003 Elliptic-hyperbolic systems and the Einstein equations *Ann. H. Poincaré* **4** 1–34
- [28] Brandt A 1977 Multilevel adaptive solutions to boundary value problems *Math. Comput.* **31** 333–390
- [29] Briggs W L, Henson V E and McCormick S F 2000 *A Multigrid Tutorial* 2nd ed (SIAM)
- [30] Kreiss H O and Lorenz J 1989 *Initial–Boundary Value Problems and the Navier–Stokes Equations* (Academic Press)
- [31] Kreiss H O, Gustafsson B and Olinger J 1995 *Time Dependent Problems and Difference Methods* (Wiley & Sons)
- [32] Boyd J P 2001 *Chebyshev and Fourier Spectral Methods* 2nd ed (Dover publications)
- [33] Penrose R 1965 Zero rest-mass fields including gravitation: Asymptotic behaviour *Proc. Royal Soc. London A* **284** 159–203
- [34] Frauendiener J 2004 Conformal infinity *Living Rev. Relativity* **7**(1)
- [35] Sarbach O and Tiglio M 2012 Continuum and discrete initial-boundary value problems and Einstein’s field equations *Living Rev. Relativity* **15**(9)
- [36] Bondi H, van der Burg M G J and Metzner A W K 1962 Gravitational waves in general relativity VII. Waves from axi-symmetric isolated systems *Proc. Royal Soc. London A* **269** 21–52
- [37] Kreiss H O, Reula O, Sarbach O and Winicour J 2007 Well-posed initial-boundary value problem for the harmonic Einstein equations using energy estimates *Class. Quantum Grav.* **24** 5973–5984
- [38] Kreiss H O and Winicour J 2006 Problems which are well-posed in a generalized sense with applications to the Einstein equations *Class. Quantum Grav.* **16** S405–S420
- [39] Ruiz M, Rinne O and Sarbach O 2007 Outer boundary conditions for Einstein’s field equations in harmonic coordinates *Class. Quantum Grav.* **24** 6349–6377
- [40] Teukolsky S A 1982 Linearized quadrupole waves in general relativity and the motion of test particles *Phys. Rev. D* **26** 745–750
- [41] Buchman L T and Sarbach O C A 2006 Towards absorbing outer boundaries in general relativity *Class. Quantum Grav.* **23** 6709–6744
- [42] Buchman L T and Sarbach O C A 2007 Improved outer boundary conditions for Einstein’s field equations *Class. Quantum Grav.* **24** S307–S326
- [43] Sarbach O and Tiglio M 2001 Gauge-invariant perturbations of Schwarzschild black holes in horizon-penetrating coordinates *Phys. Rev. D* **64** 084016
- [44] Bayliss A and Turkel E 1980 Radiation boundary conditions for wave-like equations *Commun. Pure Appl. Math.* **33** 707–725
- [45] Rinne O 2009 Explicit solution of the linearized Einstein equations in the transverse-traceless gauge for all multipoles *Class. Quantum Grav.* **26** 048003
- [46] Friedrich H 1983 Cauchy problems for the conformal vacuum field equations in general relativity *Commun. Math. Phys.* **91** 445–472
- [47] Husa S 2003 Numerical relativity with the conformal field equations *Lect. Notes Phys.* **617** 159–192
- [48] Beyer F, Doulis G, Frauendiener J and Whale B 2012 Numerical space-times near space-like and null infinity. The spin-2 system on Minkowski space *Class. Quantum Grav.* **29** 245013

- [49] Friedrich H 1998 Gravitational fields near space-like and null infinity *J. Geom. Phys.* **24** 83–163
- [50] Andersson L, Chruściel P T and Friedrich H 1992 On the regularity of solutions to the Yamabe equation and the existence of smooth hyperboloidal initial data for Einstein’s field equations *Commun. Math. Phys.* **149** 587–612
- [51] Bardeen J M and Buchman L T 2012 Bondi-Sachs energy-momentum for the constant mean extrinsic curvature initial value problem *Phys. Rev. D* **85** 064035
- [52] Rinne O 2005 *Axisymmetric Numerical Relativity* PhD thesis University of Cambridge <http://www.arxiv.org/abs/gr-qc/0601064>
- [53] Rinne O 2008 Constrained evolution in axisymmetry and the gravitational collapse of prolate Brill waves *Class. Quantum Grav.* **25** 135009
- [54] Price R H 1972 Nonspherical perturbations of relativistic gravitational collapse. I. scalar and gravitational perturbations *Phys. Rev. D* **5** 2419–2439
- [55] Pürrer M, Husa S and Aichelburg P C 2005 News from critical collapse: Bondi mass, tails, and quasinormal modes *Phys. Rev. D* **71** 104005
- [56] Pürrer M and Aichelburg P C 2009 Tails for the Einstein-Yang-Mills system *Class. Quantum Grav.* **26** 035004